Sara Pollock, Leo G. Rebholz*, and Mengying Xiao

Acceleration of nonlinear solvers for natural convection problems

https://doi.org/10.1515/jnma-2020-0067

Received September 17, 2020; revised October 23, 2020; accepted October 23, 2020

Abstract: This paper develops an efficient and robust solution technique for the steady Boussinesq model of non-isothermal flow using Anderson acceleration applied to a Picard iteration. After analyzing the fixed point operator associated with the nonlinear iteration to prove that certain stability and regularity properties hold, we apply the authors' recently constructed theory for Anderson acceleration, which yields a convergence result for the Anderson accelerated Picard iteration for the Boussinesq system. The result shows that the leading term in the residual is improved by the gain in the optimization problem, but at the cost of additional higher order terms that can be significant when the residual is large. We perform numerical tests that illustrate the theory, and show that a 2-stage choice of Anderson depth can be advantageous. We also consider Anderson acceleration applied to the Newton iteration for the Boussinesq equations, and observe that the acceleration allows the Newton iteration to converge for significantly higher Rayleigh numbers that it could without acceleration, even with a standard line search.

Keywords: Anderson acceleration, Boussinesq equations, Picard iteration, finite element method

MSC: 65B05, 65N30, 76D05

1 Introduction

Flows driven by natural convection (bouyancy) occur in many practical problems including ventilation, solar collectors, insulation in windows, cooling in electronics, and many others [9]. Such phenomena are typically modeled by the Boussinesq system, which is given in a domain $\Omega \subset \mathbb{R}^d$ (d = 2 or 3) by

$$u_{t} + (u \cdot \nabla)u - \nu \Delta u + \nabla p = \operatorname{Ri}\langle 0, \vartheta \rangle^{T} + f$$

$$\nabla \cdot u = 0$$

$$\vartheta_{t} + (u \cdot \nabla)\vartheta - \varkappa \Delta \vartheta = \gamma$$
(1.1)

with u representing the velocity field, p the pressure, θ the temperature (or density), and with f and γ the external momentum forcing and thermal sources. The kinematic viscosity $\nu > 0$ is defined as the inverse of the Reynolds number (Re = ν^{-1}), and the thermal conductivity κ is given by $\kappa = \mathrm{Re}^{-1}\mathrm{Pr}^{-1}$, where Pr is the Prandtl number and Ri is the Richardson number accounting for the gravitational force. Appropriate initial and boundary conditions are required to determine the system. The Rayleigh number is defined by Ra = Ri · Re² · Pr, and higher Ra leads to more complex physics as well as more difficulties in numerically solving the system.

Finding accurate solutions to the Boussinesq system requires the efficient solution of a discretized nonlinear system based on (1.1). We restrict our attention to those nonlinear systems arising from the steady Boussinesq system, since for nonlinear solvers, this is the more difficult case. In time dependent problems, for instance, linearizations may be used which allow one to avoid solving nonlinear systems [2]. If one does need to solve the nonlinear system at each time step (e.g., in cases where there are fast temporal dynamics),

Sara Pollock, Department of Mathematics, University of Florida, Gainesville, FL 32611, USA.

^{*}Corresponding author: Leo G. Rebholz, School of Mathematical and Statistical Sciences, Clemson University, Clemson SC 29634, USA. Email: rebholz@clemson.edu

then our work below is relevant, and the analysis as it is developed here generally applies as the time derivative term only improves the properties of the system. Moreover, at each time step one has access to good initial iterates to each subsequent nonlinear problem (e.g., the solution at the last time step).

We will consider the Picard iteration for solving the steady Boussinesq system: Given initial u_0 , define $u_k, \vartheta_k, k \ge 1$ by

$$(u_{k-1} \cdot \nabla)u_k - \nu \Delta u_k + \nabla p_k = \text{Ri} \langle 0, \vartheta_k \rangle^T + f$$
(1.2)

$$\nabla \cdot u_k = 0 \tag{1.3}$$

$$(u_{k-1} \cdot \nabla) \theta_k - \varkappa \Delta \theta_k = y \tag{1.4}$$

with u_k and θ_k satisfying appropriate boundary conditions. Our analysis will consider this iteration together with a finite element discretization. A critical feature of this iteration is that the momentum/mass equations are decoupled in each iteration from the energy equation. At each Picard iteration, one first solves the linear system (1.4), and then solves the linear system (1.2)–(1.3), which will be much more efficient than the Newton iteration (add $(u_k - u_{k-1}) \cdot \nabla u_{k-1}$ and $(u_k - u_{k-1}) \cdot \nabla u_{k-1}$ to the momentum and energy equations, respectively). The difficulty with the Newton iteration is that it is fully coupled: at each iteration the linear solve is for (u_k, p_k, θ_k) together. Such block linear systems can be difficult to solve since little is known about how to effectively precondition them.

The decoupled iteration (1.2)–(1.4), on the other hand, requires solving an Oseen linear system and a temperature transport system; many methods exist for effectively solving these linear systems [6, 7, 10]. However, even if each step of the decoupled iteration is fast, convergence properties for this iteration are not as good as those for the Newton iteration (provided a good initial guess). This motivates accelerating the nonlinear iteration for the decoupled scheme to achieve a method where each linear solve is fast, and which produces a sequence of iterates that converges rapidly to the solution. The purpose of this paper is to consider the decoupled Boussinesq iteration (1.2)–(1.4) together with Anderson acceleration.

Anderson acceleration [3] is an extrapolation technique which, after computing an update step from the current iterate, forms the next iterate from a linear combination of m previous iterates and update steps. The parameter *m* is referred to as the algorithmic depth of the iteration. The linear combination is chosen as the one which minimizes the norm of the m most recent update steps. The technique has increased in popularity since its efficient implementation and use on a variety of applications was described in [24], where it was also shown that in the linear case it is 'essentially equivalent' to GMRES. Convergence theory can be found in [17, 23], and its relation to quasi-Newton methods has been developed in [12, 13]. As shown in [11, 19, 20], as well as [23], the choice of norm used in the inner optimization problem plays an important role in the effectiveness of the acceleration. Local improvement in the convergence rate of the iteration can be shown if the original fixed-point iteration is contractive in a given norm. However, as further discussed in [20], the iteration does not have to be contractive for Anderson acceleration to be effective.

Herein, we extend the theory of improved convergence using Anderson acceleration to the Boussinesq system with the iteration (1.2)–(1.4), and demonstrate its efficiency on benchmark problems for natural convection. Our results show that applied in accordance with the developed theory of [20], the acceleration has a substantial and positive impact on the efficiency of the iteration, and even provides convergence when the iteration would otherwise fail.

Additionally, although the focus of the paper is for the Picard iteration (1.2)–(1.4), numerical testing of Anderson acceleration for the related Newton iteration is also performed. Anderson acceleration has been (numerically) shown on several test problems to enlarge the domain of convergence for Newton iterations. In our tests, Anderson accelerated Newton converges for significantly higher Rayleigh numbers than usual Newton, and thus similarly to a linesearch (but in our tests better), Anderson acceleration can enable convergence in Newton iterations that would otherwise fail. Compared to a converging Newton iteration, the Anderson accelerated Newton method will often converge slower since it will generally reduce the order of convergence to subquadratic in the vicinity of a solution [11, 21].

The remainder of the paper is organized as follows. In Section 2 we provide some background on a stable finite element spatial discretization for the steady Boussinesq equations, and on Anderson acceleration applied to a general fixed point iteration. In Section 3 we give a decoupled fixed point iteration for the steady Boussinesq system under the aforementioned finite element framework, and show that this iteration is Lipschitz Fréchet differentiable and satisfies the assumptions of [20]. Subsection 3.3 states the Anderson accelerated iteration specifically for, and as it is applied to the steady Boussinesg system, and presents the convergence results for this problem. In Section 4 we report on results for two application problems with varying Rayleigh number for the decoupled iteration of the steady Boussinesq system, and show that Anderson acceleration can have a notable positive impact on the convergence speed, especially for problems featuring a larger Rayleigh number. Section 5 shows numerical results for Anderson acceleration applied to the related Newton iteration.

2 Notation and mathematical preliminaries

This section will provide notation, mathematical preliminaries, and background, to allow for a smooth analysis in later sections. First, we will give function space and notational details, followed by finite element discretization preliminaries, and finally a brief review of Anderson acceleration.

The domain $\Omega \subset \mathbb{R}^d$ is assumed to be simply connected and to either be a convex polytope or have a smooth boundary. The $L^2(\Omega)$ norm and inner product will be denoted by $\|\cdot\|$ and (\cdot,\cdot) , respectively, and all other norms will be labeled with subscripts. Common boundary conditions for velocity and temperature are the Dirichlet conditions given by

$$u = g(x)$$
 on $\partial \Omega$, $T = h(x)$ on $\partial \Omega$ (2.1)

and mixed Dirichlet/Neumann conditions

$$u = g(x)$$
 on $\partial \Omega$, $T = h(x)$ on Γ_1 , $\nabla T \cdot n = 0$ on $\Omega \setminus \Gamma_1$ (2.2)

where $\Gamma_1 \subset \partial\Omega$, $|\Gamma_1| > 0$, and g(x), h(x) are given functions. For simplicity, we consider the homogeneous case where g(x) = 0 and h(x) = 0, and note that our results are extendable to the non-homogeneous case.

2.1 Mathematical preliminaries

In this subsection, we consider the system (1.2)-(1.4), coupled with the Dirichlet conditions (2.1), and present some standard results that will be used later. These results additionally hold for system (1.2)–(1.4) with the mixed boundary conditions (2.2), which can by seen by an integration by parts. The natural function spaces for velocity, pressure, and temperature are given by

$$\begin{split} X &= H_0^1(\Omega)^d := \left\{ v \in L^2(\Omega)^d : \, \nabla v \in L^2(\Omega)^{d \times d}, \, v = 0 \quad \text{on } \partial \Omega \right\} \\ Q &= L_0^2(\Omega) := \left\{ q \in L^2(\Omega) : \, \int_{\Omega} q \, \mathrm{d}x = 0 \right\} \\ W &= H_0^1(\Omega). \end{split}$$

The Poincaré inequality is known to hold in both X and W [18]: There exists $C_P > 0$ dependent only on the domain Ω satisfying

$$||v|| \leq C_P ||\nabla v||$$

for any $v \in X$ or $v \in W$.

Define the trilinear form $b: X \times X \times X \to \mathbb{R}$ such that for any $u, v, w \in X$

$$b(u, v, w) := \frac{1}{2}((u \cdot \nabla v, w) - (u \cdot \nabla w, v)).$$

The operator *b* is skew-symmetric and satisfies

$$b(u, v, v) = 0 \tag{2.3}$$

$$b(u, v, w) \leq M \|\nabla u\| \|\nabla v\| \|\nabla w\| \tag{2.4}$$

for any $u, v, w \in X$, with M depending only on Ω [18, Chapter 6]. Similarly, define $b^*: X \times W \times W \to \mathbb{R}$ such that for any $v \in X$ and $\varphi, \psi \in W$

$$b^*(\nu,\varphi,\psi) := \frac{1}{2}((\nu \cdot \nabla \varphi,\psi) - (\nu \cdot \nabla \psi,\varphi)).$$

One can easily check that b^* also satisfies (2.3)–(2.4).

We will denote by τ_h a regular, conforming triangulation of Ω with maximum element diameter h. The finite element spaces will be denoted as $X_h \subset X$, $Q_h \subset Q$, $W_h \subset W$, and we require that the (X_h, Q_h) pair satisfies the usual discrete inf-sup condition [8]. Common choices are Taylor-Hood elements [8], Scott-Vogelius elements on an appropriate mesh [5, 25, 26], or the mini element [4].

Define the discretely divergence-free subspace V_h by

$$V_h := \{ v \in X_h, \ (\nabla \cdot v_h, q_h) = 0 \quad \forall q_h \in Q_h \}. \tag{2.5}$$

Utilizing the space V_h will help simplify some of the analysis that follows. The discrete stationary Boussinesq equations for $(u, \vartheta) \in (V_h, W_h)$ can now be written in weak form as:

$$b(u, u, v) + v(\nabla u, \nabla v) = \operatorname{Ri}(\langle 0, \vartheta \rangle^{T}, v) + (f, v)$$
(2.6)

$$b^*(u, \theta, \chi) + \varkappa(\nabla \theta, \nabla \chi) = (\gamma, \chi) \tag{2.7}$$

for any $(v, \chi) \in (V_h, W_h)$. One can easily check that

$$\|\nabla u\| \leq K_1 := \operatorname{Ri} C_p^2 v^{-1} \varkappa^{-1} \|\gamma\|_{-1} + v^{-1} \|f\|_{-1}, \qquad \|\nabla \theta\| \leq K_2 := \varkappa^{-1} \|\gamma\|_{-1}$$
 (2.8)

by choosing v = u and $\chi = \theta$ in (2.6)–(2.7). We next present a set of sufficient conditions to guarantee the uniqueness of the solution for the discrete stationary Boussinesq equations. We note that K_1 and K_2 depend only on problem data and are independent of the mesh width *h*.

Lemma 2.1 (small data condition). The following are sufficient conditions for the system (2.6)-(2.7) to have a unique solution

$$v^{-1}M(2K_1 + \varkappa^{-1}MK_2^2) < 1, \qquad v^{-1}\varkappa^{-1}Ri^2C_p^4 < 1.$$
 (2.9)

The following stronger condition will also be used in the sequel in order to simplify some of the constants. Define $\eta := \min\{\nu, \kappa\}$, then by the definition of K_1 and K_2 in (2.8), we have the following inequality

$$\begin{split} \nu^{-1}M\left(2K_1 + \varkappa^{-1}MK_2^2\right) & \leq \eta^{-2}M\left(2(\mathrm{Ri}\;C_p^2\varkappa^{-1}\|\gamma\|_{-1} + \|f\|_{-1}) + \varkappa^{-2}M\|\gamma\|_{-1}^2\right) \\ & \nu^{-1}\varkappa^{-1}\mathrm{Ri}^2\;C_p^4 & \leq \eta^{-2}\mathrm{Ri}^2\;C_p^4. \end{split}$$

Then a stronger sufficient condition for uniqueness of solutions to (2.6)–(2.7) is given by

$$\eta^{-2}M\left(2(\operatorname{Ri} C_{p}^{2} \varkappa^{-1} \|\gamma\|_{-1} + \|f\|_{-1}) + \varkappa^{-2}M\|\gamma\|_{-1}^{2}\right) < 1, \qquad \eta^{-1}\operatorname{Ri} C_{p}^{2} < 1 \tag{2.10}$$

which implies κ^{-1} Ri $C_p^2 < 1$.

Proof. Assume $(u, \theta), (w, z) \in (V_h, W_h)$ are solutions to the (2.6)–(2.7). Subtracting these two systems produces

$$b(u, u - w, v) + b(u - w, w, v) + v(\nabla(u - w), \nabla v) = \operatorname{Ri}(\langle 0, \theta - z \rangle^{T}, v)$$

$$b^{*}(u, \theta - z, \chi) + b^{*}(u - w, z, \chi) + \varkappa(\nabla(\theta - z), \nabla \chi) = 0.$$

Setting v = u - w, $\chi = \theta - z$ eliminates the first nonlinear terms in both equations and yields

$$v\|\nabla(u-w)\|^{2} \leq v^{-1} \operatorname{Ri}^{2} C_{P}^{4} \|\nabla(\vartheta-z)\|^{2} + 2MK_{1} \|\nabla(u-w)\|^{2}$$
$$\varkappa\|\nabla(\vartheta-z)\|^{2} \leq \varkappa^{-1} M^{2} K_{1}^{2} \|\nabla(u-w)\|^{2}$$

thanks to Cauchy-Schwarz, Young, and Poincaré inequalities, together with (2.4) and (2.8). Combining these bounds, we obtain

Under the conditions (2.9), both terms on the left-hand side of (2.11) are nonnegative, and in fact positive unless u = w and $\theta = z$, implying the solution is unique.

In the remainder, we will assume either (2.9) or (2.10) holds, to guarantee the well-posedness of the system (2.6)–(2.7). For notational simplicity, we prefer using the stronger (2.10). All of the results in Section 3 hold as well for (2.9) with minor differences in the constants.

2.2 Anderson acceleration

The extrapolation technique known as Anderson acceleration, which is used to improve the convergence of a fixed-point iteration, may be stated as follows [23, 24]. Consider a fixed-point operator $g: Y \to Y$, where Y is a normed vector space.

Algorithm 2.1 (Anderson iteration). Anderson acceleration with depth $m \ge 0$ and damping factors $0 < \beta_k \le 1$. Step 0: Choose $x_0 \in Y$.

Step 1: Find $w_1 \in Y$ such that $w_1 = g(x_0) - x_0$. Set $x_1 = x_0 + w_1$.

Step *k*: For k = 2, 3, ... Set $m_k = \min\{k - 1, m\}$.

- (a) Find $w_k = g(x_{k-1}) x_{k-1}$.
- (b) Solve the minimization problem for $\{\alpha_i^k\}_{k=m_k}^{k-1}$

$$\min \left\| \left(1 - \sum_{j=k-m_k}^{k-1} \alpha_j^k \right) w_k + \sum_{j=k-m_k}^{k-1} \alpha_j^k w_j \right\|_{V}.$$
 (2.12)

(c) For damping factor $0 < \beta_k \le 1$, set

$$x_{k} = \left(1 - \sum_{j=k-m_{k}}^{k-1} \alpha_{j}^{k}\right) x_{k-1} + \sum_{j=k-m_{k}}^{k-1} \alpha_{j}^{k} x_{j-1} + \beta_{k} \left(\left(1 - \sum_{j=k-m_{k}}^{k-1} \alpha_{j}^{k}\right) w_{k} + \sum_{j=k-m_{k}}^{k-1} \alpha_{j}^{k} w_{j}\right)$$
(2.13)

where $w_i = g(x_{i-1}) - x_{i-1}$ may be referred to as the update step or as the nonlinear residual.

Depth m = 0 returns the original fixed-point iteration. For purposes of implementation with depth m > 0, it makes sense to write the algorithm in terms of an unconstrained optimization problem rather than a constrained problem as in (2.12) [13, 20, 24]. Define matrices E_k and F_k , whose columns are the consecutive differences between iterates and residuals, respectively:

$$E_{k-1} := (e_{k-1} \ e_{k-2} \ \cdots \ e_{k-m_k}), \quad e_j = x_j - x_{j-1}$$
 (2.14)

$$F_k := ((w_k - w_{k-1}) (w_{k-1} - w_{k-2}) \cdots (w_{k-m_k+1} - w_{k-m_k})).$$
(2.15)

Then defining $y^k = \operatorname{argmin}_{v \in \mathbb{R}^m} \| w_k - F_k y \|_V$, the update step (2.13) may be written as

$$x_k = x_{k-1} + \beta_k w_k - (E_{k-1} + \beta_k F_k) \gamma^k = x_{k-1}^{\alpha} + \beta_k w_k^{\alpha}$$
 (2.16)

where $w_k^{\alpha} = w_k - F_k \gamma^k$ and $x_{k-1}^{\alpha} = x_{k-1} - E_{k-1} \gamma^k$ are the averages corresponding to the solution from the optimization problem. The optimization gain factor ξ_k may be defined by

$$\|w_k^{\alpha}\| = \xi_k \|w_k\|. \tag{2.17}$$

The gain factor ξ_k plays a critical role in the recent theory [11, 20] that shows how this acceleration technique improves convergence. Specifically, the acceleration reduces the contribution from the first-order residual term by a factor of ξ_k , but introduces higher-order terms into the residual expansion of the accelerated iterate.

The next two assumptions, summarized from [20], give sufficient conditions on the fixed point operator g, for the analysis presented there to hold.

Assumption 2.1. Assume $g \in C^1(Y)$ has a fixed point x^* in Y, and there are positive constants C_0 and C_1 with

- 1. $||g'(x)|| \le C_0$ for all $x \in Y$, and
- 2. $||g'(x) g'(y)|| \le C_1 ||x y||$ for all $x, y \in Y$.

Assumption 2.2. Assume there is a constant $\sigma > 0$ for which the differences between consecutive residuals and iterates satisfy

$$||w_{k+1} - w_k||_Y \ge \sigma ||x_k - x_{k-1}||_Y, \quad k \ge 1.$$

Under Assumptions 2.1 and 2.2, the following result summarized from [20] produces a one-step bound on the residual $\|w_{k+1}\|$ in terms of the previous residual $\|w_k\|$. This result supposes the sufficient linear independence of the columns of each matrix F_j given by (2.15), in the following sense. Denote the direction cosine between two vectors u and v be given by $\cos(u,v)=(u,v)/(\|u\|\|v\|)$. Denote the nonnegative direction sine between u and v as $|\sin(u,v)|=\sqrt{1-\cos^2(u,v)}$, and the direction sine between u and the subspace spanned by $\{v_1,\ldots v_m\}$ as

$$|\sin(u, \operatorname{span}\{v_1, \dots, v_m\})| = \sqrt{1 - \cos(u, v_1)^2 - \cos(u, v_2)^2 - \dots - \cos(u, v_m)^2}.$$

Denoting column i of matrix F_j as $f_{j,i}$, for $i=1,\ldots,m_j$, the direction sines between each $f_{j,i}$ and the subspace spanned by $f_{j,1},\ldots,f_{j,i-1}$, will be assumed bounded below by a constant $c_s>0$. As discussed in [20], this assumption can be both verified and ensured, so long as the optimization problem of Algorithm 3.1 is solved in a norm induced by an inner-product (as it is in the present setting), in which case it can be solved as a least-squares problem using a (thin) QR decomposition as in [15]. Concisely, if $F_j=QR$, then $|\sin(f_{j,i}, \operatorname{span}\{f_{j,1},\ldots f_{j,i-1}\})|=r_{ii}/\|f_{j,i}\|$. In terms of a safeguarding strategy, columns of F_j (and, respectively, E_{j-1}) where the desired inequality fails to hold can be removed. This method is demonstrated in [20], (see also similar filtering strategies used in [1, 16, 24]) but was not found necessary in the present numerical results.

Theorem 2.1 (Pollock, Rebholz, 2019). Let Assumptions 2.1 and 2.2 hold, and suppose the direction sines between each column i of F_j defined by (2.15) and the subspace spanned by the preceding columns satisfies $|\sin(f_{j,i}, \operatorname{span}\{f_{j,1}, \ldots, f_{j,i-1}\})| \ge c_s$ for some constant $c_s > 0$, for $j = k - m_k, \ldots, k-1$. Then the residual $w_{k+1} = g(x_k) - x_k$ from Algorithm 2.1 (depth m) satisfies the following bound

$$\|w_{k+1}\| \leq \|w_k\| \left(\xi_k((1-\beta_k) + C_0\beta_k) + \frac{1}{2}CC_1\sqrt{1-\theta_k^2} \right)$$

$$\times \left(\|w_k\| h(\xi_k) + 2 \sum_{n=k-m_k+1}^{k-1} (k-n) \|w_n\| h(\xi_n) + m_k \|w_{k-m_k}\| h(\xi_{k-m_k}) \right)$$
(2.18)

where each $h(\xi_j) \leq C\sqrt{1-\xi_j^2} + \beta_j \xi_j$, and C depends on c_s and the implied upper bound on the direction cosines.

The one-step estimate (2.18) shows how the relative contributions from the lower and higher order terms are determined by the gain ξ_k from the optimization problem. The lower order terms are scaled by ξ_k and the higher-order terms are scaled by $\sqrt{1-\xi_k^2}$. Greater algorithmic depths m generally give smaller values of ξ_k as the optimization is run over an expanded search space. However, the reduction comes at the cost of both increased accumulation and weight of higher order terms. If recent residuals are small, then this may be negligible and greater algorithmic depths m may be advantageous (to a point). If the previous residual terms are large however (e.g., near the beginning of an iteration), then greater depths m may slow or prevent convergence in many cases.

3 A decoupled fixed point iteration for the Boussinesq system

All results in this section hold for both Dirichlet boundary conditions (2.1), and mixed boundary conditions (2.2), with minor differences in the constants. We will use the Dirichlet boundary conditions for illustration. One can easily extend the analysis for the mixed boundary conditions.

We will consider the following fixed point iteration: Given u_0 , θ_0 , for k = 1, 2, 3, ..., find $(u_k, p_k, \theta_k) \in (X_h, Q_h, W_h)$ satisfying for all $v \in X_h$, $q \in Q_h$, and $\chi \in W_h$,

$$b(u_{k-1}, u_k, v) + \nu(\nabla u_k, \nabla v) - (p_k, \nabla \cdot v) = \operatorname{Ri}\left(\langle 0, \theta_k \rangle^T, v \rangle + (f, v)\right)$$
(3.1)

$$(\nabla \cdot u_k, q) = 0 \tag{3.2}$$

$$b^*(u_{k-1}, \theta_k, \chi) + \varkappa(\nabla \theta_k, \nabla \chi) = (\gamma, \chi). \tag{3.3}$$

For finite element spaces X_h , Q_h satisfying the discrete inf-sup condition as described in subsection 2.1, we have the equivalent formulation in the discretely divergence-free space (2.5): for any $v \in V_h$ and $\chi \in W_h$,

$$b(u_{k-1}, u_k, v) + v(\nabla u_k, \nabla v) = \operatorname{Ri}\left(\langle 0, \theta_k \rangle^T, v\right) + (f, v)$$
(3.4)

$$b^*(u_{k-1}, \theta_k, \chi) + \varkappa(\nabla \theta_k, \nabla \chi) = (y, \chi). \tag{3.5}$$

The following subsections develop a framework which will allow us to analyze this iteration.

3.1 A solution operator G corresponding to the fixed point iteration

We will consider the solution operator of the system (3.4)–(3.5) as the fixed-point operator defining the iteration to be accelerated. To study this operator, we next formally define it in a slightly more abstract way.

Given $f \in H^{-1}(\Omega)^d$, $\gamma \in H^{-1}(\Omega)$, and $(u, \vartheta) \in (V_h, W_h)$, consider the problem of finding $(\tilde{u}, \tilde{\vartheta}) \in (V_h, W_h)$ satisfying

$$b(u, \tilde{u}, v) + v(\nabla \tilde{u}, \nabla v) = \text{Ri}\left(\langle 0, \tilde{\vartheta} \rangle^T, v\right) + (f, v)$$
(3.6)

$$b^*(u,\widetilde{\vartheta},\chi) + \varkappa(\nabla\widetilde{\vartheta},\nabla\chi) = (\chi,\chi) \tag{3.7}$$

for any $v \in V_h$ and $\chi \in W_h$.

Lemma 3.1. For $f \in H^{-1}(\Omega)^d$ and $\gamma \in H^{-1}(\Omega)$, the system (3.6)–(3.7) is well-posed, and solutions satisfy the bounds

$$\|\nabla \widetilde{u}\| \le K_1, \qquad \|\nabla \widetilde{\vartheta}\| \le K_2$$
 (3.8)

where K_1 and K_2 are given in (2.8).

Proof. We begin with *a priori* bounds. Suppose solutions exist, and choose $\chi = \tilde{\vartheta}$ and $v = \tilde{u}$. By construction, this vanishes the trilinear terms in each equation. After applying Cauchy–Schwarz, Poincaré, and Hölder inequalities, it can be seen that

$$\begin{split} & \nu \|\nabla \widetilde{u}\|^2 \leq \operatorname{Ri} C_P^2 \|\nabla \widetilde{\vartheta}\| \|\nabla \widetilde{u}\| + \|f\|_{-1} \|\nabla \widetilde{u}\| \\ & \varkappa \|\nabla \widetilde{\vartheta}\|^2 \leq \|\gamma\|_{-1} \|\nabla \widetilde{\vartheta}\|. \end{split}$$

The second bound reduces to $\|\nabla \tilde{\theta}\| \le \kappa^{-1} \|y\|_{-1}$, and inserting this into the first bound produces

$$\|\nabla \widetilde{u}\| \leq \text{Ri } C_P^2 v^{-1} \varkappa^{-1} \|y\|_{-1} + v^{-1} \|f\|_{-1}.$$

Since the system (3.6)–(3.7) is linear in \tilde{u} and $\tilde{\theta}$, and finite dimensional, these bounds are sufficient to imply solution uniqueness and therefore existence.

Definition 3.1. Define $G:(V_h,W_h)\to (V_h,W_h)$ to be the solution operator of (3.6)–(3.7). That is,

$$(\widetilde{u},\widetilde{\theta})=G(u,\theta).$$

By Lemma 3.1, G is well defined. The Boussinesq fixed point iteration (3.4)–(3.5) can now be written as

$$(u_k, \theta_k) = G(u_{k-1}, \theta_{k-1}).$$

Definition 3.2. Define the norm $\|(\cdot,\cdot)\|_B:(V_h,W_h)\to\mathbb{R}$ by

$$\|(v, w)\|_B := \sqrt{v\|\nabla v\|^2 + \varkappa \|\nabla w\|^2}.$$

The weights used in the norm definition come from the natural norm of the Boussinesq system, and this norm will be referred to as the B-norm. This weighted norm is used since it arises naturally out of the analysis, and our analysis suggests it is the natural norm to use for the optimization step of the accelerated algorithm.

3.2 Continuity and Lipschitz differentiability of G

We now prove that *G* satisfies Assumptions 2.1 and 2.2. We begin with Lipschitz continuity.

Lemma 3.2. There exists a positive constant C_G such that $||G(u, \theta) - G(w, z)||_B \le C_G ||(u, \theta) - (w, z)||_B$ for any $(u, \theta), (w, z) \in (V_h, W_h)$. The constant C_G is defined by

$$C_G = v^{-1/2} \eta^{-1/2} M \sqrt{2K_1^2 + 3K_2^2}.$$

Proof. For any $(u, \theta) \in (V_h, W_h)$, denote $(G_1(u, \theta), G_2(u, \theta))$ as the components of $G(u, \theta)$. Let $(u, \theta), (w, z) \in (V_h, W_h)$. Set $G(u, \theta) = (G_1(u, \theta), G_2(u, \theta))$ and $G(w, z) = (G_1(w, z), G_2(w, z))$. Then for all $(v, \chi) \in (V_h, W_h)$ we have

$$b(u, G_1(u, \theta), v) + v(\nabla G_1(u, \theta), \nabla v) = \operatorname{Ri}\left(\langle 0, G_2(u, \theta)\rangle^T, v\right) + (f, v)$$
(3.9)

$$b^*(u, G_2(u, \theta), \chi) + \varkappa(\nabla G_2(u, \theta), \nabla \chi) = (\gamma, \chi)$$
(3.10)

$$b(w, G_1(w, z), v) + v(\nabla G_1(w, z), \nabla v) = \text{Ri}(\langle 0, G_2(w, z) \rangle^T, v) + (f, v)$$
(3.11)

$$b^*(w, G_2(w, z), \chi) + \varkappa(\nabla G_2(w, z), \nabla \chi) = (\gamma, \chi).$$
(3.12)

Subtracting (3.11)–(3.12) from (3.9)–(3.10) gives

$$b(u, G_1(u, \theta) - G_1(w, z), v) + b(u - w, G_1(w, z), v) + v(\nabla(G_1(u, \theta) - G_1(w, z)), \nabla v)$$

$$= \text{Ri}(\langle 0, G_2(u, \theta) - G_2(w, z) \rangle^T, v)$$
(3.13)

$$b^*(u, G_2(u, \theta) - G_2(w, z), \chi) + b^*(u - w, G_2(w, z), \chi) + \varkappa(\nabla(G_2(u, \theta) - G_2(w, z)), \nabla\chi) = 0$$
(3.14)

Choosing $\chi = G_2(u, \theta) - G_2(w, z)$ in (3.14) eliminates the first term, then applying (2.4) and (3.8) gives

$$\|\nabla (G_2(u,\theta) - G_2(w,z))\| \le \kappa^{-1} M K_2 \|\nabla (u-w)\|. \tag{3.15}$$

Similarly, choosing $v = G_1(u, \theta) - G_1(w, z)$ in (3.13) eliminates the first nonlinear term, and applying (2.4), Hölder and Poincaré inequalities produces

$$\|\nabla(G_{1}(u,\theta) - G_{1}(w,z))\| \leq v^{-1} \operatorname{Ri} C_{p}^{2} \|\nabla(G_{2}(u,\theta) - G_{2}(w,z))\| + v^{-1} M \|\nabla(u-w)\| \|\nabla G_{1}(w,z)\|$$

$$\leq v^{-1} M(\kappa^{-1} K_{2} \operatorname{Ri} C_{p}^{2} + K_{1}) \|\nabla(u-w)\|$$

$$\leq v^{-1} M(K_{1} + K_{2}) \|\nabla(u-w)\|$$
(3.16)

thanks to (3.8) of Lemma 3.1 and (2.10). Combining (3.15)–(3.16) gives

$$||G(u, \theta) - G(w, z)||_B \le v^{-1/2} \eta^{-1/2} M \sqrt{2K_1^2 + 3K_2^2} ||(u, \theta) - (w, z)||_B.$$

Thus *G* is Lipschitz continuous with constant
$$C_G = v^{-1/2} \eta^{-1/2} M \sqrt{2K_1^2 + 3K_2^2}$$
.

Next, we show that G is Lipschitz Fréchet differentiable. We will first define a mapping G', and then in Lemma 3.3 confirm that it is the Fréchet derivative operator of G.

Definition 3.3. Given $(u, \vartheta) \in (V_h, W_h)$, define an operator $G'(u, \vartheta; \cdot, \cdot) : (V_h, W_h) \to (V_h, W_h)$ by

$$G'(u, \theta; h, s) := (G'_1(u, \theta; h, s), G'_2(u, \theta; h, s))$$

satisfying for all $(h, s), (v, \chi) \in (V_h, W_h)$

$$b(h, G_1(u, \theta), v) + b(u, G'_1(u, \theta; h, s), v) + v(\nabla G'_1(u, \theta; h, s), \nabla v) = \text{Ri}(\langle 0, G'_2(u, \theta; h, s) \rangle^T, v)$$
(3.17)

$$b^{*}(h, G_{2}(u, \theta), \chi) + b^{*}(u, G_{2}'(u, \theta; h, s), \chi) + \varkappa(\nabla G_{2}'(u, \theta; h, s), \nabla \chi) = 0.$$
(3.18)

Once it is established that G' is well-defined and is the Fréchet derivative of G, it follows that $G'(u, \theta; \cdot, \cdot)$ is the Jacobian matrix of G at (u, ϑ) . From the partially decoupled system (3.17)–(3.18), it is clear that $G'(u, \vartheta; \cdot, \cdot)$ is a block upper triangular matrix. Applied to any $(h, s) \in (V_h, W_h)$, the resulting $G'(u, \theta; h, s)$ can be written componentwise as $(G'_1(u, \theta; h, s), G'_2(u, \theta; h, s)) \in (V_h, W_h)$.

Lemma 3.3. The Boussinesq operator G is Lipschitz Fréchet differentiable: there exists a constant \hat{C}_G such that for all (u, θ) , (w, z), $(h, s) \in (V_h, W_h)$

$$\|G'(u, \theta; h, s)\|_{B} \le C_{G}\|(h, s)\|_{B}$$
 (3.19)

and

$$\|G'(u+h, \theta+s; w, z) - G'(u, \theta; w, z)\|_{B} \le \widehat{C}_{G} \|(h, s)\|_{B} \|(w, z)\|_{B}$$
(3.20)

where C_G is defined in Lemma 3.2.

Proof. The first part of the proof shows that *G* is Fréchet differentiable, and (3.19) holds. We begin by finding an upper bound on the norm of G' and then showing G' is well-defined. Setting $\chi = G'_2(u, \theta; h, s)$ in (3.18) eliminates the second nonlinear term and gives

$$\|\nabla G_2'(u, \theta; h, s)\| \le \kappa^{-1} M \|\nabla h\| \|\nabla G_2(u, \theta)\| \le \kappa^{-1} M K_2 \|\nabla h\|$$
(3.21)

thanks to Lemma 3.1. Similarly, setting $v = G'_1(u, \theta; h, s)$ in (3.17) eliminates the second nonlinear term and yields

$$\|\nabla G_{1}'(u, \theta; h, s)\| \leq v^{-1} \operatorname{Ri} C_{p}^{2} \|\nabla G_{2}'(u, \theta; h, s)\| + v^{-1} M \|\nabla h\| \|\nabla G_{1}(u, \theta)\|$$

$$\leq v^{-1} M (u^{-1} K_{2} \operatorname{Ri} C_{p}^{2} + K_{1}) \|\nabla h\|$$

$$\leq v^{-1} M (K_{1} + K_{2}) \|\nabla h\|$$
(3.22)

thanks to Lemma 3.1, (3.21), and the small data condition (2.10). Combining the bounds (3.21)–(3.22) yields

$$||G'(u, \theta; h, s)||_{B} \le C_{G}||(h, s)||_{B}.$$
 (3.23)

Since system (3.17)–(3.18) is linear and finite dimensional, (3.23) is sufficient to imply the system is well-posed. Therefore, G' is well-defined and uniformly bounded over (V_h, W_h) , since the bound is independent of (u, θ) .

Next, we prove G' given by Definition 3.3 is the Fréchet derivative operator of G. That is, given $(u, \theta) \in$ (V_h, W_h) , there exists some constant C such that for any $(h, s) \in (V_h, W_h)$

$$||G(u+h, \theta+s) - G(u, \theta) - G'(u, \theta; h, s)||_{B} \le C||(h, s)||^{2}.$$

For notational ease, set $\tilde{g}_1 = G_1(u+h, \vartheta+s) - G_1(u, \vartheta) - G_1'(u, \vartheta; h, s)$ and $\tilde{g}_2 = G_2(u+h, \vartheta+s) - G_2(u, \vartheta) - G_2(u, \vartheta)$ $G'_2(u, \theta; h, s)$. To construct the left hand side of the inequality above, we begin with the following equations: for any (u, θ) , (h, s), $(v, \chi) \in (V_h, W_h)$

$$b(u+h, G_1(u+h, \theta+s), v) + v(\nabla G_1(u+h, \theta+s), \nabla v) = \text{Ri}((0, G_2(u+h, \theta+s))^T, v) + (f, v)$$
(3.24)

$$b^*(u+h,G_2(u+h,\vartheta+s),\chi) + \varkappa(\nabla G_2(u+h,\vartheta+s),\nabla\chi) = (\gamma,\chi)$$
(3.25)

$$b(u, G_1(u, \theta), v) + v(\nabla G_1(u, \theta), \nabla v) = \operatorname{Ri}\left(\langle 0, G_2(u, \theta)\rangle^T, v\right) + (f, v) \tag{3.26}$$

$$b^*(u, G_2(u, \theta), \chi) + \varkappa(\nabla G_2(u, \theta), \nabla \chi) = (\gamma, \chi). \tag{3.27}$$

Subtracting (3.24)–(3.25) from (3.26)–(3.27) and (3.17)–(3.18), and then choosing $v = \tilde{g}_1, \chi = \tilde{g}_2$, we obtain by application of (2.4), Hölder and Sobolev inequalities [18, Ch. 6] that

$$\begin{split} \nu\|\nabla\widetilde{g}_1\|^2 &= -b(h,G_1(u+h,\vartheta+s)-G_1(u,s),\widetilde{g}_1) + \mathrm{Ri}\left(\langle 0,\widetilde{g}_2\rangle^T,\widetilde{g}_1\right) \\ &\leq M\|\nabla h\|\|\nabla(G_1(u+h,\vartheta+s)-G_1(u,\vartheta)\|\|\nabla\widetilde{g}_1\| + \mathrm{Ri}\,C_P^2\|\nabla\widetilde{g}_2\|\|\nabla\widetilde{g}_1\| \\ \varkappa\|\nabla\widetilde{g}_2\|^2 &= -b(h,G_2(u+h,\vartheta+s)-G_2(u,\vartheta),\widetilde{g}_2) \end{split}$$

which reduces to

$$\kappa \|\nabla \tilde{g}_2\|^2 \leq \kappa^{-1} M^2 \|\nabla h\|^2 \|\nabla (G_2(u+h, \theta+s) - G_2(u, \theta))\|^2$$
(3.28)

and

$$v\|\nabla \tilde{g}_{1}\|^{2} \leq 2v^{-1}M^{2}\|\nabla h\|^{2} (\|\nabla (G_{1}(u+h,\theta+s)-G_{1}(u,\theta)\|^{2} + \operatorname{Ri}^{2} C_{P}^{4} \kappa^{-2} \|\nabla (G_{2}(u+h,\theta+s)-G_{2}(u,\theta))\|^{2})$$

$$\leq 2\eta^{-1}v^{-1}M^{2}\|\nabla h\|^{2}\|\nabla (G(u+h,\theta+s)-G(u,\theta))\|_{B}^{2}$$
(3.29)

thanks to Young's inequality and (2.10). Combining bounds (3.28)-(3.29) produces

$$\|(\widetilde{g}_1,\widetilde{g}_2)\|_B^2 \leq 3\eta^{-2}M^2\|\nabla h\|^2\|\nabla (G(u+h,\vartheta+s)-G(u,\vartheta))\|_B^2 \leq 3\eta^{-3}M^2C_G^2\|(h,s)\|_B^4.$$

By the definitions of \tilde{g}_1 , \tilde{g}_2 , this shows

$$\|G(u+h, \theta+s) - G(u, \theta) - G'(u, \theta; h, s)\|_{B} \le 2\eta^{-3/2} M C_{G} \|(h, s)\|_{B}^{2}$$
(3.30)

which demonstrates Fréchet differentiability of G at (u, θ) . As (3.30) holds for arbitrary (u, θ) , we have that G is Fréchet differentiable on all of (V_h, W_h) .

The second part of the proof shows that G' is Lipschitz continuous over (V_h, W_h) . By the definition of G', the following equations hold

$$b(w, G_1(u, \theta), v) + b(u, G'_1(u, \theta; w, z), v) + v(\nabla G'_1(u, \theta; w, z), \nabla v) = \text{Ri}(\langle 0, G'_2(u, \theta; w, z) \rangle^T, v)$$
(3.31)

$$b^{*}(w, G_{2}(u, \theta), \chi) + b^{*}(u, G_{2}'(u, \theta; w, z), \chi) + \varkappa(\nabla G_{2}'(u, \theta; w, z), \nabla \chi) = 0$$
(3.32)

$$b(w, G_1(u+h, \theta+s), v) + b(u+h, G'_1(u+h, \theta+s; w, z), v) + v(\nabla G'_1(u+h, \theta+s; w, z), \nabla v) = \text{Ri}(\langle 0, G'_2(u+h, \theta+s; w, z) \rangle^T, v)$$
(3.33)

$$b^*(w, G_2(u+h, \theta+s), \chi) + b^*(u+h, G_2'(u+h, \theta+s; w, z), \chi) + \varkappa(\nabla G_2'(u+h, \theta+s; w, z), \nabla \chi) = 0$$
 (3.34)

for all (u, θ) , (w, z), (h, s), $(v, \chi) \in (V_h, W_h)$. Letting $e_1 := G'_1(u + h, \theta + s; w, z) - G'_1(u, \theta; w, z)$, $e_2 := G'_2(u + h, \theta + s; w, z) - G'_2(u, \theta; w, z)$ and subtracting (3.31)–(3.32) from (3.33)–(3.34) gives

$$b(w, G_1(u+h, \theta+s) - G_1(u, \theta), v) + b(h, G'_1(u, \theta; w, z), v) + b(u+h, e_1, v) + v(\nabla e_1, \nabla v) = \text{Ri}(\langle 0, e_2 \rangle^T, v)$$

$$b^*(w, G_2(u+h, \vartheta+s) - G_2(u, \vartheta), \chi) + b^*(h, G_2'(u, \vartheta; w, z), \chi) + b^*(u+h, e_2, \chi) + \varkappa(\nabla e_2, \nabla v) = 0.$$

Setting $v = e_1$, $\chi = e_2$ eliminates the last nonlinear terms in both equations and produces

$$v\|\nabla e_{1}\|^{2} \leq \operatorname{Ri} C_{P}^{2}\|\nabla e_{2}\|\|\nabla e_{1}\| + M\|\nabla w\|\|\nabla (G_{1}(u+h,\vartheta+s) - G_{1}(u,\vartheta))\|\|\nabla e_{1}\|$$

$$+ M\|\nabla h\|\|\nabla G_{1}'(u,\vartheta;w,z)\|\|\nabla e_{1}\|$$

$$\varkappa \|\nabla e_2\|^2 \leq M \|\nabla w\| \|\nabla (G_2(u+h,\vartheta+s) - G_2(u,\vartheta))\| \|\nabla e_2\| + M \|\nabla h\| \|\nabla G_2'(u,\vartheta;w,z)\| \|\nabla e_2\|$$

thanks to (2.4). Thus from (3.15)-(3.16), (3.21)-(3.22), (3.23), and Lemma 3.2, we obtain

$$\begin{split} \|\nabla e_2\| &\leq 2M^2 \varkappa^{-2} K_2 \|\nabla w\| \|\nabla h\| \\ \|\nabla e_1\| &\leq \nu^{-1} \mathrm{Ri} \ C_p^2 \|\nabla e_2\| + 2\nu^{-2} M^2 (K_1 + K_2) \|\nabla h\| \nabla w\| \\ &\leq 2\nu^{-1} \eta^{-1} M^2 (K_1 + 2K_2) \|\nabla w\| \|\nabla h\|. \end{split}$$

Combing these bounds gives

$$\|(e_1,e_2)\|_B^2 \leq 4 v^{-2} \eta^{-3} M^4 (2K_1^2 + 9K_2^2) \|(h,s)\|_B^2 \|(w,z)\|_B^2 = \widehat{C}_G^2 \|(h,s)\|_B^2 \|(w,z)\|_B^2$$

where $\widehat{C}_G = 2\nu^{-1}\eta^{-3/2}M^2(2K_1^2 + 9K_2^2)^{1/2}$ is the Lipschitz constant of G'. Thus $G'(u, \theta; \cdot, \cdot)$ is Lipschitz continuous with constant \widehat{C}_G . As the bound holds for arbitrary (u, θ) , we have that G is Lipschitz continuously differentiable on (V_h, W_h) with constant \widehat{C}_G .

It remains to show that Assumption 2.2 is satisfied for the solution operator *G*. This amounts to finding a constant $\sigma > 0$ such that for any (u, θ) , $(w, z) \in (V_h, W_h)$ with $\|\nabla u\|$, $\|\nabla w\| \leq K_1$

$$||F(u, \theta) - F(w, z)||_{B} \ge \sigma ||(u, \theta) - (w, z)||_{B}$$
 (3.35)

where $F(u, \theta) := G(u, \theta) - (u, \theta)$.

Lemma 3.4. Assume the problem data is such that G is contractive, i.e., $C_G < 1$. Then there exists a constant $\sigma > 0$ such that (3.35) holds for any (u, θ) , $(w, z) \in (V_h, W_h)$ with $\|\nabla u\|$, $\|\nabla w\| \leq K_1$.

Proof. Since *G* is contractive, it follows from [20, Remark 4.2] that (3.35) holds with
$$\sigma = 1 - C_G$$
.

This shows that Assumption 2.2 is satisfied under the data restriction that $C_G < 1$, which is similar but not equivalent to the uniqueness conditions in Section 2. However, in our numerical tests, which used data far larger than these restrictions, the σ_k 's calculated at each iteration (i.e., (3.35) with $u = u_k$, $\theta = \theta_k$, $w = u_{k-1}$, $z = g_{k-1}$) were in general no smaller than 10^{-3} . Hence it may be possible to prove that Assumption 2.2 holds under less restrictive data restrictions.

3.3 Accelerating the decoupled Boussinesg iteration

In this section, we provide the algorithm of Anderson acceleration applied to the decoupled Boussinesq system (3.4)–(3.5) with either Dirichlet (2.1) or mixed boundary conditions (2.2). The one-step residual bound is stated below for Boussinesq solve operators *G*.

Algorithm 3.1 (Anderson accelerated iterative method for Boussinesq equations).

Step 0: Give an initial $u_0 \in X_h$, $\theta_0 \in W_h$.

Step 1a: Find $\tilde{\theta}_1 \in W_h$ satisfying for all $\chi \in W_h$

$$b^*(u_0, \widetilde{\vartheta}_1, \chi) + \varkappa(\nabla \widetilde{\vartheta}_1, \nabla \chi) = (\gamma, \chi).$$

Step 1b: Find $\tilde{u}_1 \in V_h$ satisfying for all $v \in V_h$

$$b(u_0, \tilde{u}_1, v) + v(\nabla \tilde{u}_1, \nabla v) = \text{Ri}\left(\langle 0, \tilde{\vartheta}_1 \rangle^T, v\right) + (f, v).$$

Then set $u_1 = \tilde{u}_1$, $\theta_1 = \tilde{\theta}_1$, and $w_1 = \tilde{u}_1 - u_0$, $z_1 = \tilde{\theta}_1 - \theta_0$.

Step k: For $k = 2, 3, ..., \text{ set } m_k = \min\{k - 1, m\}.$

(a) Find $\tilde{\theta}_k \in W_h$ by solving

$$b^*(u_{k-1}, \widetilde{\vartheta}_k, \chi) + \varkappa(\nabla \widetilde{\vartheta}_k, \nabla \chi) = (\gamma, \chi). \tag{3.36}$$

(b) Find $\tilde{u}_k \in V_h$ by solving

$$b(u_{k-1}, \widetilde{u}_k, \nu) + \nu(\nabla \widetilde{u}_k, \nabla \nu) = \text{Ri}(\langle 0, \widetilde{\vartheta}_k \rangle^T, \nu) + (f, \nu)$$
(3.37)

and then compute $w_k = \tilde{u}_k - u_{k-1}$, $z_k = \tilde{\theta}_k - \theta_{k-1}$.

(c) Solve the minimization problem

$$\min \|(w_k^{\alpha}, z_k^{\alpha})\|_B \tag{3.38}$$

for
$$\{\alpha_i^k\}_{j=k-m_k}^{k-1}$$
, where $(w_k^{\alpha}, z_k^{\alpha}) := \left(1 - \sum_{j=k-m_k}^{k-1} \alpha_j^k\right)(w_k, z_k) + \sum_{j=k-m_k}^{k-1} \alpha_j^{k+1}(w_j, z_j)$.

(d) For damping factor $0 < \beta_k \le 1$, set

$$(u_k, \theta_k) = \left(1 - \sum_{j=k-m_k}^{k-1} \alpha_j^k\right) (u_{k-1}, \theta_{k-1}) + \sum_{j=k-m_k}^{k-1} \alpha_j^k (u_{j-1}, \theta_{j-1}) + \beta_k \left(\left(1 - \sum_{j=k-m_k}^{k-1} \alpha_j^k\right) (w_k, z_k) + \sum_{j=k-m_k}^{k-1} \alpha_j^{k+1} (w_j, z_j)\right).$$

As the Boussinesq operator G satisfies Assumptions 2.1 and 2.2, we have the following convergence result of Algorithm 3.1 by directly applying Theorem 5.5 from [20].

Theorem 3.1 (convergence result for Algorithm 3.1). The k-th step residual (w_k, z_k) generated from Algorithm 3.1 satisfies

$$\begin{aligned} \|(w_{k+1}, z_{k+1})\|_{B} &\leq \|(w_{k}, z_{k})\|_{B} \left(\xi_{k} (1 - \beta_{k} + \widehat{K}_{g} \beta_{k}) + \frac{1}{2} C \widehat{C}_{G} \sqrt{1 - \xi_{k}^{2}} \left(\|(w_{k}, z_{k})\|_{B} h(\xi_{k}) \right. \\ &+ 2 \sum_{j=k-m_{k}+1}^{k-1} (k-j) \|(w_{j}, z_{j})\|_{B} h(\xi_{j}) + m_{k-1} \|(w_{k-m_{k}}, z_{k-m_{k}})\|_{B} h(\xi_{k-m_{k}}) \right) \end{aligned}$$

where $\xi_k := \|(w_k^{\alpha}, z_k^{\alpha})\|_B / \|(w_k, z_k)\|_B$, $h(\xi_j) \leq C\sqrt{1 - \xi_j^2} + \beta_j \xi_j$, and C depends on a lower bound of the direction sine between $(w_{j+1}, z_{j+1}) - (w_j, z_j)$ and span $\{(w_{n+1}, z_{n+1}) - (w_n, z_n)\}_{n=j-m_k+1}^{j-1}$.

4 Numerical experiments for Anderson accelerated Picard iterations

We now demonstrate the Anderson accelerated Picard iteration for the Boussinesq system on two test problems, a benchmark differentially heated cavity problem on the unit square and a related problem with a more complex domain. For both problems, we observe a significant increase in convergence speed resulting from Anderson acceleration, in particular for larger Rayleigh numbers.

4.1 Differentially heated cavity

Our first test problem is the differentially heated cavity problem from [9], with varying Rayleigh number. The domain for the problem is the unit square, and for boundary conditions we enforce no slip velocity on all walls, $\nabla T \cdot n = 0$ on the top and bottom, and T(1, y) = 1, T(0, y) = 0. The initial iterates $u_0 = 0$ and $T_0 = 0$, are used for all tests. No continuation method or pseudo time stepping is employed.

The discretization uses $(P_2, P_1^{\rm disc})$ velocity–pressure Scott–Vogelius elements, and P_2 temperature elements. The mesh is created by starting with a uniform triangulation, refining along the boundary, then applying a barycenter refinement (Alfeld split, in the language of Fu, Guzman, and Neilan [14]). The resulting mesh is shown in Fig. 1, and with this element choice provides 89,554 total degrees of freedom. We show results below for varying Rayleigh numbers, which come from using parameters $\nu=0.01$ and $\mu=0.01$, and varying Ri. Plots of resolved solutions for varying Ra are shown in Fig. 2.

In our tests, we consider both constant algorithmic depths m, and also a 2-stage strategy that uses a smaller m (1 or 2) when the nonlinear residual is larger than 10^{-3} in the B-norm, and m=20 when the residual is smaller. The 2-stage approach is motivated by Theorem 3.1, which suggests that greater depths m can be detrimental early in the iteration due to the accumulation of non-negligible higher order terms in the residual expansion. Once the residual is sufficiently small, then the reduction of the first order terms from a greater depth m can be enjoyed without noticeable pollution from the higher-order terms, which essentially results in an improved linear convergence rate.

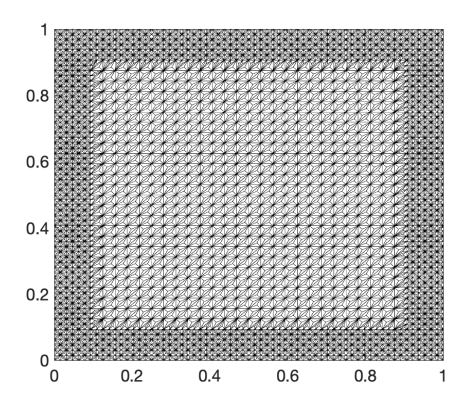


Fig. 1: The mesh used for numerical tests.

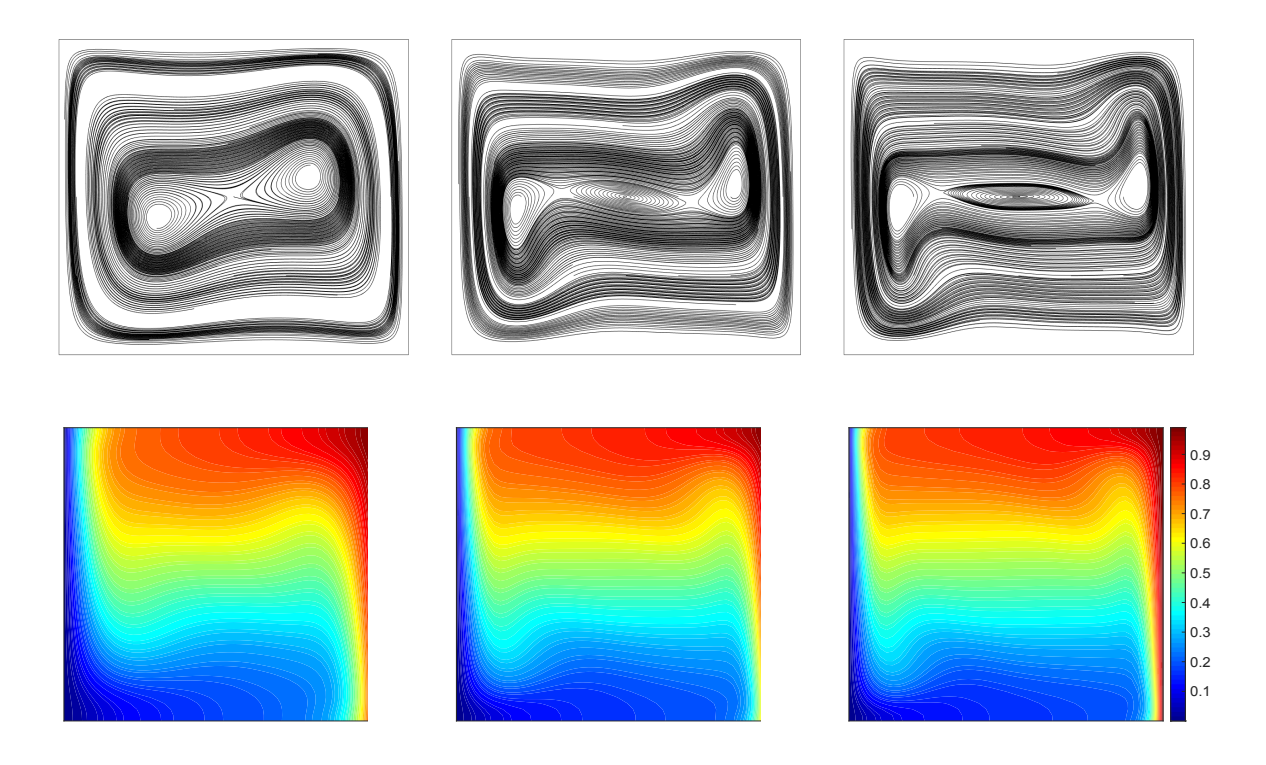


Fig. 2: The resolved solution's velocity streamlines (top) and temperature contours (bottom), for $Ra = 10^5$, $5 \cdot 10^5$, and 10^6 , from left to right.

We test here Algorithm 3.1, i.e., the Anderson accelerated Picard iteration for the Boussinesq system, for varying choices of depth m and damping parameter β , and for several Rayleigh numbers: Ra = 10^5 , 5 · 10^5 , 10^6 , $2 \cdot 10^6$. For each Ra, we tested with m = 0 (no acceleration) and each fixed damping parameter $\beta = 0.05, 0.1, 0.15, \dots, 1$, and then used the best β from all tests with that Ra. Respectively, for Ra = 10^5 , 5. 10^5 , 10^6 , $2 \cdot 10^6$, these parameters were $\beta = 0.3$, 0.05, 0.05, 0.05. Although we did not systematically check that the optimal β for m = 0 was necessarily optimal for nonzero m, several preliminary tests did indicate that this β should generally be a good choice. In these results, we did not monitor or enforce sufficient linear independence of the columns of the matrix used in the least-squares problem (see the discussion above Theorem 2.1); however, even with m = 20 we saw fast convergence once the residual was small enough, so this was not deemed necessary. Convergence results for varying m are shown in Fig. 3, displayed in terms of

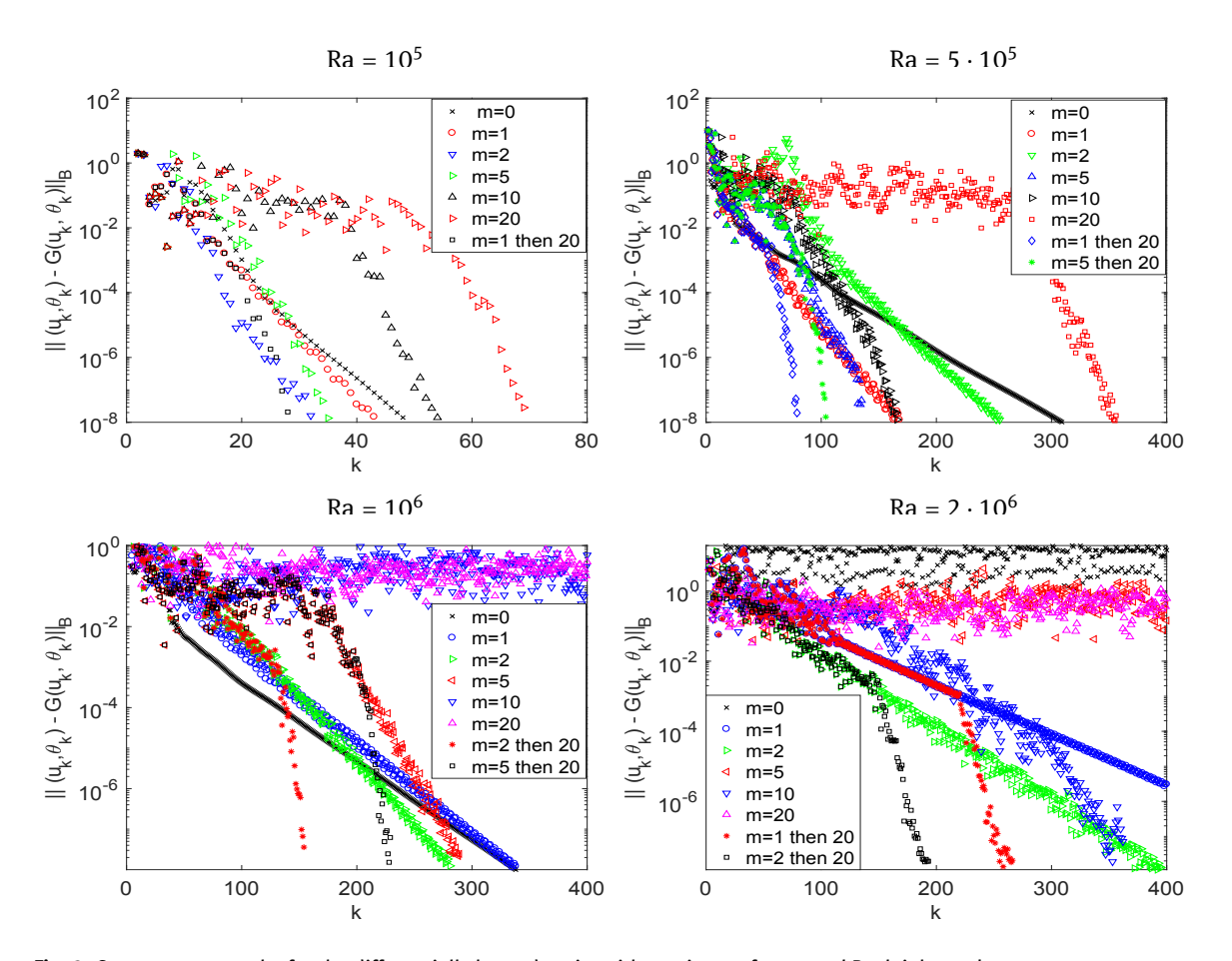


Fig. 3: Convergence results for the differentially heated cavity with varying m, for several Rayleigh numbers.

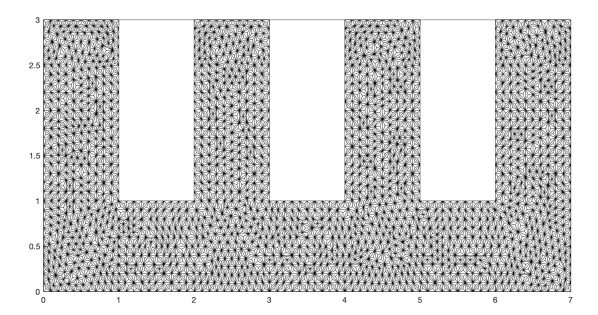
the B-norm of the nonlinear residual versus iteration number. We note that the usual Picard iteration, i.e., m=0 and $\beta=1$, did not converge for any of these Ra numbers; after 500 iterations, the B-norm was still larger than 10^{-1} . With the appropriately chosen relaxation parameters, the Picard iteration did converge for each case except when Ra = $2 \cdot 10^6$.

Convergence results for the lowest Rayleigh number, Ra = 10^5 , are shown in the top left of Fig. 3 for different values of m and fixed $\beta = 0.3$. Here, we observe the unaccelerated method converges rather quickly, and the accelerated methods that converged faster were m = 1 and m = 2 and the 2-stage method that uses m = 1 and then switches to m = 20, with the 2-stage method giving the best results. Anderson accelerated Picard with m = 5, 10, 20 all converged, but slower than if no acceleration was used.

Results for Ra = $5 \cdot 10^5$ also show lower values of m improving convergence but higher values slowing convergence. Indeed, m = 1, 2, 5 along with 2-stage methods that used m = 1 then 20 and m = 5 then 20, all outperformed the unaccelerated iteration, while m = 10 and m = 20 slowed convergence. For Ra = 10^6 , the methods with smaller constant m = 1, 2, 5 converged, all in roughly the same number of iterations as the unaccelerated method, while the methods run with larger m = 10, 20 did not converge within 400 iterations. Once again, significant improvement is seen from using 2-stage choices of m, and this gave the best results.

With Ra = $2 \cdot 10^6$, results showed more improvement from the acceleration, as compared to those with lower Ra. Here, the unaccelerated Picard iteration did not converge, and neither does the iteration with m = 1. Again, the best results come from using a 2-stage choice of m, using a lesser depth at the beginning of the iteration, and a greater depth once the residual is sufficiently small.

The results described above show a clear advantage from using Anderson acceleration with the Picard iteration, especially for larger Rayleigh numbers. These results are also in good agreement with our theory, which demonstrates that Anderson acceleration decreases the first order term but then adds higher order



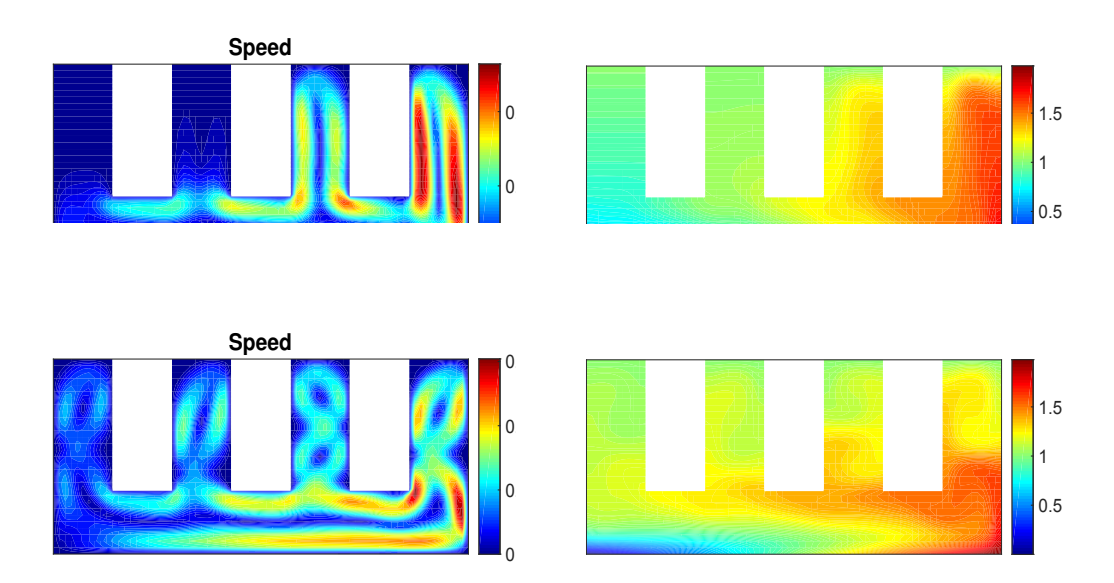


Fig. 5: Plots above show the speed (left) and temperature (right) of the solution for the second numerical test, using Rayleigh numbers $Ra = 10^4$ (top) and $5 \cdot 10^4$ (bottom).

terms to the residual bound. Hence using greater algorithmic depths when the residual is large can sufficiently pollute the solution so that the improvement found in the reduction of the first order term is outweighed by the additional contributions from higher order terms. In all cases, m = 10, 20 slowed convergence compared to m = 0, if the m = 0 iteration converged. Both theory and these experiments also suggest that early in the iteration, moderate choices of algorithmic depth can be advantageous. The best results shown here come from the 2-stage strategy, which takes advantage of the reduction in the first-order residual term, but only once the residual is small enough that the higher-order contributions are negligible in comparison.

4.2 Differentially heated complex domain

We now present results from a second test that has a more complex domain (see Fig. 4). For temperature boundary conditions, we use T(x, 1) = 1, T(x, 0) = 2x/7, and $\nabla T \cdot n = 0$ on all other boundaries. The velocity boundary conditions are no-slip on all walls. We use a barycenter refined uniform triangulation mesh, together with (P_2, P_1^{disc}) Scott–Vogelius velocity–pressure elements, and P_2 for temperature which provides 70,068 total degrees of freedom. We use parameters v = 0.01, $\kappa = 0.01$, and then choose the Richardson number Ri to create Rayleigh numbers Ra = 10^4 and $5 \cdot 10^4$; plots of resolved solutions are shown in Fig. 5.

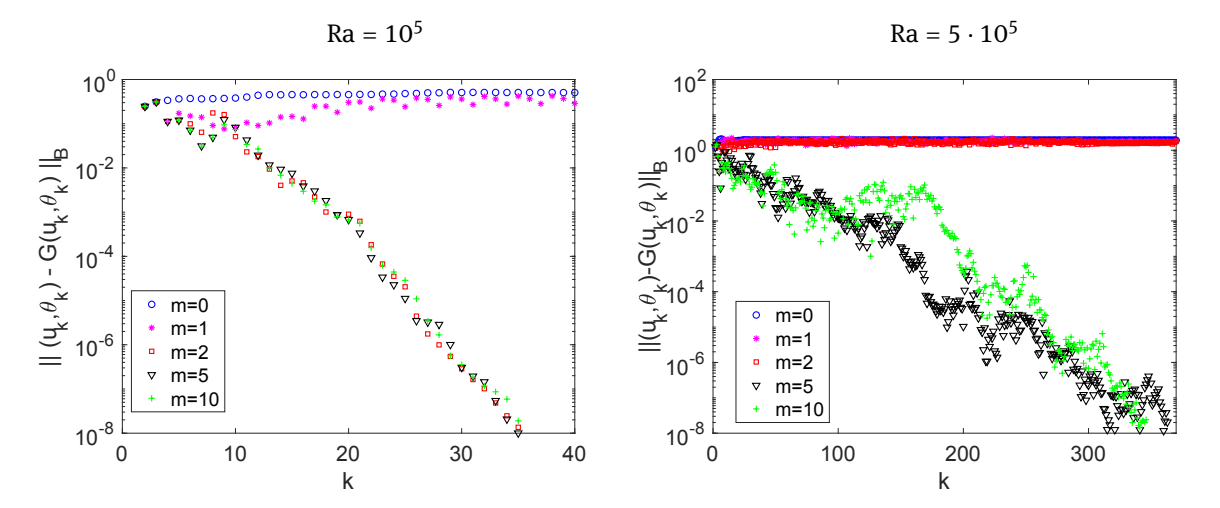


Fig. 6: Convergence plots of Anderson accelerated Picard iteration with Rayleigh numbers Ra = 10^4 (left) and $5 \cdot 10^4$ (right), with Anderson depth m = 0, 1, 2, 5, 10.

For each Ra, we run the Anderson accelerated Picard iteration using varying m and $\beta = 1$. Plots for convergence are shown in Fig. 6, and in both cases we observe that the unaccelerated Picard iteration (m = 0) fails to converge, as does m = 1. For Ra = 10^4 , tests with $m \ge 2$ all converged, and m = 2, 5, 10 converged at about the same rate. For Ra = $5 \cdot 10^4$, m = 2 fails but m = 5 and m = 10 both converge. As in the previous test, Anderson acceleration enables convergence of the Picard iteration if it is applied with a sufficiently large algorithmic depth m. However, if the depth is too great, pollution from earlier iterates interferes with convergence, at least until the error is sufficiently small. This can be seen in Fig. 6 by the reduced regularity in the earlier stages of convergence with m = 10, as compared with m = 5.

5 Acceleration of the Newton iteration for the Boussinesq system

While the theory for this paper focuses on the Picard iteration, it is also of interest to consider the Newton iteration for the Boussinesq system, which takes the form

$$(u_{k-1} \cdot \nabla)u_k + (u_k \cdot \nabla)u_{k-1} - (u_{k-1} \cdot \nabla)u_{k-1} - \nu \Delta u_k + \nabla p_k = \operatorname{Ri} \langle 0, \vartheta_k \rangle^T + f$$
(5.1)

$$\nabla \cdot u_k = 0 \tag{5.2}$$

$$(u_{k-1} \cdot \nabla) \vartheta_k + (u_k \cdot \nabla) \vartheta_{k-1} - (u_{k-1} \cdot \nabla) \vartheta_{k-1} - \varkappa \Delta \vartheta_k = y \tag{5.3}$$

together with appropriate boundary conditions.

The Newton iteration is often superior for solving nonlinear problems, particularly if one can find an initial guess sufficiently close to a solution. However, for Boussinesq systems, the Newton iteration also comes with a significant additional difficulty in that the linear systems that need to be solved at each iteration are fully coupled. That is, one needs to solve larger block linear systems for (u_k, p_k, ϑ_k) simultaneously, whereas for the Picard iteration one first solves for ϑ_k , and then solves a Navier–Stokes type system for (u_k, p_k) . Hence each iteration of Picard is significantly more efficient than each iteration of Newton.

We proceed now to test Anderson acceleration applied to the Newton iteration, using the same differentially heated cavity problem and discretization studied above. While theory to describe how Anderson acceleration can improve the performance of Newton iterations has yet to be developed, evidence for the efficacy of the method has been described in [11, 21]. While the acceleration can be expected to interfere with Newton's quadratic convergence in the vicinity of a solution, the advantage explored here is the behavior of the algorithm outside of that regime. In the far-field regime, outside the domain of asymptotically quadratic convergence, the Newton iteration may converge linearly [22], or, of course, not at all. In compar-

Tab. 1: Iterations required for Anderson accelerated Newton iterations to converge, with $\beta = 1$ and varying m. Results of the unaccelerated Newton method with line searches are also shown.

Ri	Ra	<i>m</i> = 0	<i>m</i> = 1	<i>m</i> = 2	<i>m</i> = 5	<i>m</i> = 10	m = 0 + LS1	m = 0 + LS2
1	1e+4	9	9	11	14	17	7	7
10	1e+5	В	17	19	81	38	В	11
20	2e+5	В	В	В	34	36	В	20
50	5e+5	В	В	В	44	56	В	В
100	1e+6	В	В	В	В	В	В	В
150	1.5e+6	В	В	В	В	В	В	В
200	2e+6	В	В	В	В	В	В	В

Tab. 2: Iterations required for Anderson accelerated Newton iterations to converge to a nonlinear residual of 10^{-8} in the Bnorm, with $\beta = 0.3$ and varying m. 'B' denotes the nonlinear residual growing above 10^4 , and 'F' denotes no convergence after 200 iterations.

Ri	Ra	<i>m</i> = 0	<i>m</i> = 1	<i>m</i> = 2	<i>m</i> = 5	<i>m</i> = 10
1	1e+4	13	11	10	11	13
10	1e+5	В	18	18	23	52
20	2e+5	В	41	32	22	44
50	5e+5	В	В	В	74	134
100	1e+6	В	В	В	95	F
150	1.5e+6	В	В	В	В	141
200	2e+6	В	В	В	В	156

ing accelerated Newton with Newton augmented with a line search, we demonstrate how the acceleration can effectively enlarge the domain of convergence for Newton iterations. As shown in the experiments below, a damped accelerated Newton iteration with algorithmic depth m = 10 can also solve the Boussinesq system with Ra = $2 \cdot 10^6$.

In the following tests, convergence was declared if the nonlinear residual fell below 10^{-8} in the B-norm. If residuals grew larger than 10⁴ in the B-norm, the iteration was terminated, and the test was declared to fail due to (essentially) blowup, and is denoted with a 'B' in the tables below. If an iteration did not converge within 200 iterations but its residuals all stayed below 10⁴ in the B-norm, we declared it to be a failure and denote it with an 'F' in the tables below.

We first tested Anderson acceleration applied to the Newton iteration, with varying m and no relaxation $(\beta = 1)$. Results are shown in Table 1, and a clear improvement can be seen in convergence for higher Ra as mincreases. For comparison, we also show results of (unaccelerated) Newton with a line search, and give results from two choices of line searches: LS1 continuously cuts the Newton step size ratio in half (up to 1/64), until either finding a step that decreases the nonlinear residual of the finite element problem, or using a step size ratio of 1/64 otherwise. LS2 uses 'fminbnd' from MATLAB (golden section search and parabolic interpolation) to use the step size ratio from [0.01,1] that minimizes the nonlinear residual of the finite element problem. While the line searches do help convergence of the Newton iteration, they do not perform as well as Newton-Anderson (m = 5 or 10) for higher Ra values.

We next considered Anderson acceleration to Newton, but using relaxation of $\beta = 0.3$. Result are shown in Table 2, and we observe further improvement compared to the case of $\beta = 1$. Lastly, we considered Anderson acceleration applied to Newton, but choosing the β from $\{0.0625, 0.125, 0.25, 0.5, 1\}$ that has the smallest residual in the B-norm. This is essentially a look-ahead step, which increases the cost of each step of the accelerated Newton algorithm by a factor of 4. Results from choosing β this way were significantly better than for constant $\beta = 1$, and somewhat better than $\beta = 0.3$, although not worth the extra cost except when using $\beta = 0.3$ failed. A clear conclusion for this section is that Anderson acceleration with a properly chosen depth and relaxation can significantly improve the ability for the Newton iteration to converge for larger Ra.

Tab. 3: Iterations required for Anderson accelerated Newton iterations to converge to a nonlinear residual of 10^{-8} in the B-norm, with β being chosen as the best from a set of five values, and varying m. 'B' denotes the nonlinear residual growing above 10^4 , and 'F' denotes no convergence after 200 iterations.

Ri	Ra	<i>m</i> = 0	<i>m</i> = 1	<i>m</i> = 2	<i>m</i> = 5	<i>m</i> = 10
1	1e+4	8	9	9	13	24
10	1e+5	F	13	14	20	38
20	2e+5	123	21	27	32	61
50	5e+5	35	59	31	65	93
100	1e+6	В	42	F	68	106
150	1.5e+6	В	В	В	F	112
200	2e+6	В	В	В	F	150

6 Conclusions and future directions

In this paper, we studied Anderson acceleration applied to the Picard iteration for Boussinesq system. The Picard iteration is advantageous compared to the Newton iteration for this problem because it decouples the linear systems into easier to solve pieces. Since convergence of Picard iterations is typically slow, it is a good candidate for acceleration. In this work we showed that the Anderson acceleration analysis framework developed in [20] was applicable to this Picard iteration, by considering each iteration as the application of a particular solution operator, and then proving the solution operator had the required properties laid out in [20]. This in turn proved one-step error analysis results from [20] hold for Anderson acceleration applied to the Boussinesq system, and local convergence of the accelerated method under a small data condition. Numerical tests with the 2D differentially heated cavity problem showed good numerical results demonstrating the convergence behavior was consistent with our theory, and in particular that a 2-stage choice of Anderson depth works very well. Anderson acceleration applied to the related Newton iteration was also considered in numerical tests and it was found that Anderson acceleration allowed for convergence at significantly higher Rayleigh numbers than the usual Newton iteration with common line search techniques.

For future work, we plan to consider more sophisticated ways to choose m adaptively. For the Picard iteration, the 2-stage choice of m (small m early and larger m later) was rather crude but yet very effective and so we expect a more sophisticated method based on our analysis should work even better. For the Newton iteration, adaptively choosing m in a different way than Picard (m small at first and then m=0 later) could be beneficial since Anderson can help Newton converge when far from a root but can slow convergence when near a root. Optimally and adaptively choosing β at each step is also an important problem we plan to consider. Being able to quasi-optimally and adaptively choose m and β in a systematic way will allow for Anderson acceleration to be automated and thus be more easily and successfully used.

Funding: The author SP acknowledges support from National Science Foundation through the grant DMS 2011519. The author LR acknowledges support from National Science Foundation through the grant DMS 2011490.

References

- [1] H. An, X. Jia, and H. F. Walker, Anderson acceleration and application to the three-temperature energy equations. *J. Comput. Phys.* **347** (2017), 1–19.
- [2] M. Akbas, S. Kaya, and L. Rebholz, On the stability at all times of linearly extrapolated BDF2 timestepping for multiphysics incompressible flow problems. *Num. Meth. P.D.E.s* **33** (2017), No. 4, 995–1017.
- [3] D. G. Anderson. Iterative procedures for nonlinear integral equations. J. Assoc. Comput. Mach. 12 (1965), No. 4, 547–560.
- [4] D. Arnold, F. Brezzi, and M. Fortin, A stable finite element for the Stokes equations. Calcolo 21 (1984), No. 4, 337-344.

- D. Arnold and J. Qin, Quadratic velocity/linear pressure Stokes elements. In: Advances in Computer Methods for Partial Differential Equations VII (Eds. R. Vichnevetsky, D. Knight, and G. Richter), IMACS, 1992, pp. 28-34.
- M. Benzi, G. Golub, and J. Liesen, Numerical solution of saddle point problems. Acta Numerica 14 (2005), 1–137.
- M. Benzi and M. Olshanskii, An augmented Lagrangian-based approach to the Oseen problem. SIAM J. Sci. Comput. 28 (2006), 2095-2113.
- S. Brenner and L. R. Scott, The Mathematical Theory of Finite Element Methods, 3rd edition. Springer-Verlag, 2008.
- [9] A. Cibik and S. Kaya, A projection-based stabilized finite element method for steady state natural convection problem. J. Math. Anal. Appl. 381 (2011), 469-484.
- [10] H. Elman, D. Silvester, and A. Wathen, Finite Elements and Fast Iterative Solvers with applications in incompressible fluid dynamics. Numerical Mathematics and Scientific Computation, Oxford Univ. Press, Oxford, 2014.
- [11] C. Evans, S. Pollock, L. Rebholz, and M. Xiao, A proof that Anderson acceleration increases the convergence rate in linearly converging fixed point methods (but not in quadratically converging ones). SIAM J. Numer. Anal. 58 (2020), 788-810.
- [12] V. Eyert, A comparative study on methods for convergence acceleration of iterative vector sequences. J. Comput. Phys. 124 (1996), No. 2, 271-285.
- [13] H. Fang and Y. Saad, Two classes of multisecant methods for nonlinear acceleration. Numer. Linear Algebra Appl. 16 (2009), No. 3, 197-221.
- [14] G. Fu, J. Guzman, and M. Neilan, Exact smooth piecewise polynomial sequences on Alfeld splits. Math. Comput. 89 (2020), No. 323, 1059-1091,
- [15] G. H. Golub, C. F. Van Loan, Matrix Computations, 3rd ed. Johns Hopkins University Press, Baltimore, 1996.
- [16] R. Haelterman, A. E. J. Bogaers, K. Scheufele, B. Uekermann, and M. Mehl, Improving the performance of the partitioned QN-ILS procedure for fluid-structure interaction problems: filtering. Comput. Struct. 171 (2016), 9-17.
- [17] C.T. Kelley, Numerical methods for nonlinear equations. Acta Numerica 27 (2018), 207-287.
- [18] W. Layton, An Introduction to the Numerical Analysis of Viscous Incompressible Flows. SIAM, Philadelphia, 2008.
- [19] S. Pollock, L. Rebholz, and M. Xiao, Anderson-accelerated convergence of Picard iterations for incompressible Navier-Stokes equations. SIAM J. Numer. Anal. 57 (2019), No. 2, 615-637.
- [20] S. Pollock and L. G. Rebholz, Anderson acceleration for contractive and noncontractive iterations. IMA J. Numer. Anal. 41 (2021), No.4, 2841-2872
- [21] S. Pollock and H. Schwartz, Benchmarking results for the Newton-Anderson method. Results Appl. Math. 8 (2020), 100095, 1-11.
- [22] V. Pták, The rate of convergence of Newton's process. Numer. Math. 25 (1976), 279-285.
- [23] A. Toth and C. T. Kelleyr, Convergence analysis for Anderson acceleration. SIAM J. Numer. Anal. 53 (2015), No. 2, 805-819.
- [24] H. F. Walker and P. Ni. Anderson acceleration for fixed-point iterations. SIAM I. Numer. Anal. 49 (2011), No. 4, 1715–1735.
- [25] S. Zhang, A new family of stable mixed finite elements for the 3D Stokes equations. Math. Comp. 74 (2005), No. 250, 543-
- [26] S. Zhang, A family of $Q_{k+1,k} \times Q_{k,k+1}$ divergence-free finite elements on rectangular grids. SIAM J. Numer. Anal. 47 (2009), No. 3, 2090-2107.